Stress–strain behaviour of a clayey silt in triaxial tests

Dayarathne, R.S., Hawlader B.C.
Memorial University, St. John's, NL, Canada

GEOQuébec 2015
Challenges from North to South
Des défis du Nord au Sud

ABSTRACT
Frost heave is one the major issues in the design of pipelines in cold regions. The pipelines generally traverse through a variety of soils. Among the different types of soil, clayey silt has been identified as one of the highly frost susceptible soils. In the analyses of pipeline–soil interaction due to frost heave, the stress–strain behaviour of both unfrozen and unfrozen soil is equally important. In the current research program, centrifuge physical modeling and finite element analysis will be performed to examine the effects of frost heave on chilled gas pipelines. While a large number of laboratory test results on different sands and clays are available in the literature, laboratory tests on clayey silt, which is highly frost susceptible, are very limited. In this paper, some triaxial and consolidation test results on clayey silt are presented, which could be used to understand its constitutive behaviour. The soil used in this experimental program is same as the soil used for centrifuge physical modeling. Comparing test results with typical behaviour of sand and clay in the critical state framework, some similarity and differences are highlighted.

RÉSUMÉ
Le soulèvement par le gel est l'un des enjeux majeurs de la conception des pipelines dans les régions froides. Les pipelines traversent généralement une variété de sols. Parmi les différents types de sol, le silt argileux a été identifié comme l'un des plus susceptibles au gel. Dans les analyses d'interaction pipelines-sol dû au soulèvement par le gel, le comportement contrainte-déformation est aussi important pour le cas de sol non-gelé que pour le cas gelé. Dans le programme de recherche en cours, le modelage physique par centrifugeuse et l'analyse par éléments finis seront effectués, pour observer les effets du soulèvement par le gel sur les pipelines à gaz froid. Alors qu'un grand nombre de résultats provenant des tests en laboratoire sur les sables et les argiles sont disponibles, les tests sur les silts argileux sont très limités. Dans cet article, des tests triaxiaux et de consolidation sur le silt argileux, pouvant être utilisés pour comprendre son comportement constitutif, sont présentés. Le sol utilisé dans le programme expérimental est le même que celui utilisé pour la centrifugeuse. En comparant les résultats des tests avec le comportement typique du sable et de l'argile dans le cadre d'un état critique, quelques similarités et différences ressortent.

1 INTRODUCTION

Frost heave is a process in which soil freezing causes moisture flow. It has significant effects on the design of chilled gas pipelines that pass through variety of soils along its route. All types of soil are not frost susceptible. Previous studies showed that clayey silt is one of the highly frost susceptible soil (Andersland and Ladanyi 2004). Various attempts have been taken in the past to understand the mechanisms involved in frost heave and its effects on pipeline design. Based on one-dimensional model test results, frost heave models have been proposed by a number of researchers (Konrad and Morgenstern 1984; Nixon 1991). Large-scale tests, such as Calgary full-scale test, Caen frost heave test, have been also conducted in the past to improve the knowledge and design methodologies of large-diameter chilled gas pipelines in discontinuous permafrost. Physical modeling of frost heave has been also conducted using geotechnical centrifuge, which is less expensive than full-scale tests (Ketcham et al. 1997; Yang and Goodings 1998; Clark and Philips 2003; Morgan et al. 2004; Morgan et al. 2006; Piercey et al. 2011).

The mathematical models developed from model test results have been also implemented in numerical models for analysis of frost heave. For example, the Segregation Potential (SP) model proposed by Konrad and Morgenstern (1984) has implemented in a FE code (Konrad and Shen 1996) and finite difference code (Nixon 1991). The stress–strain behaviour of both frozen and unfrozen soil influences the response of pipeline subjected to frost heave, which has to be given in numerical models. The stress–strain behaviour of unfrozen soil is the focus of the present study. Most of the previous studies assumed that unfrozen soil behaves as an elastic material (Konrad and Shen 1996; Ladanyi and Shen 1993; Michalowski and Zhu 2006, Shen and Ladanyi 1991). In a recent study, Nishimura et al. (2009) used the critical state model to simulate the response of both frozen and unfrozen soil as shown in Fig. 1. In this model, the yield surface expands with decrease in temperature below the freezing point.

At this stage, a question is whether clayey silt, which is highly frost susceptible, behaves elastically for the range of stress around the pipeline, and/or they also follow the critical state framework as suggested by Nishimura et al. (2009). Although limited, some recent studies (e.g. Nocilla et al. 2006) showed that the silt behaves as '*transitional materials'* in one-dimensional and triaxial loading conditions.

In the present research program, physical and numerical modeling will be performed to understand better the frost heave mechanisms under chilled gas pipelines. In the following section, a brief introduction of frost heave modeling using geotechnical centrifuge is given first. After that a series of laboratory consolidation and triaxial tests results on the soil used for these centrifuge tests are presented to examine the constitutive behaviour of this soil in unfrozen condition.

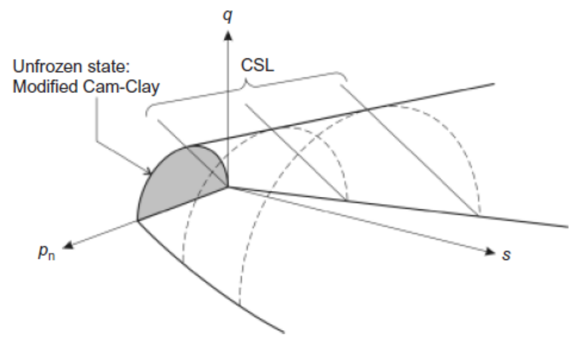

Figure 1. Critical state model for frozen and unfrozen soils (Nishimura et al. 2009)

2 CENTRIFUGE MODELING OF FROST HEAVE UNDER CHILLED GAS PIPELINES

A number of centrifuge tests have been performed in the past for frost heave modeling of chilled gas pipelines using the geotechnical centrifuge at C-CORE. It has been shown that the centrifuge test results are consistent with the full-scale test results (Clark and Philips 2003; Morgan et al. 2004; Piercey et al. 2011). In addition to tests on natural frost susceptible soils, a large number of tests have been conducted on Sil-Co-Sil silt and kaolin mix. Based on these centrifuge modeling and one-dimensional frost heave tests, it is found that 75% Sil-Co-Sil silt and 25% kaolin mix are highly frost susceptible. A typical section after a centrifuge frost heave test is shown in Fig. 2. As shown, significant heave occurred with formation of ice lenses. Outside the frozen bulb the soil is unfrozen. The stress–strain behaviour of the unfrozen soil is investigated in the following sections.

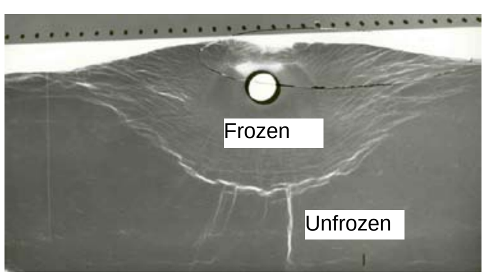

Figure 2. Typical section after centrifuge modeling of frost heave

3 ONE-DIMENSIONAL CONSOLIDATION AND TRIAXIAL TESTS

3.1 Material and Sample Preparation

Two identical reconstituted cylindrical soil blocks were prepared from a mixture of 25% Speswhite kaolin and 75% Sil-Co-Sil silt. The particle size distribution of each material and the mixture are shown in Fig. 3. According to the unified soil classification system this clayey silt can be classified as ML. Other properties of the mixture are summarized in Table 1.

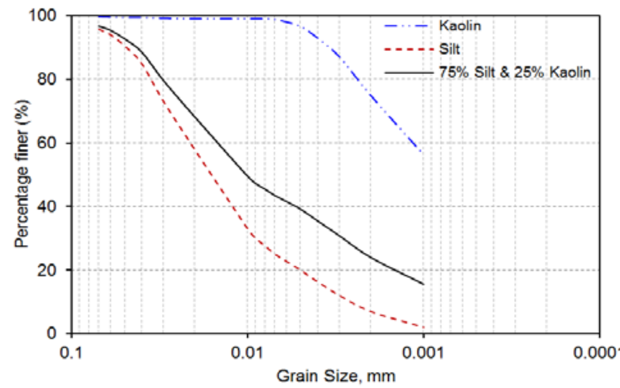

Figure 3. Grain size distributions of materials

By adding water twice the liquid limit (LL) of the mixture, uniform slurry was prepared by thoroughly mixing in a drum type machine mixer for 2 hours, which was then poured into a cylindrical consolidation tub of 300 mm diameter and 350 mm height. Appropriate care was taken to prevent segregation and air entrapping by reducing the drop height and pouring the slurry in three layers with a slight stirring at each layer. The sample was then consolidated on the laboratory floor by applying a vertical pressure from a piston, so that the soil was strong enough to handle. A number of soil samples were then collected from this laboratory floor consolidated soil block using a Shelby tube. The samples were then extruded and the specimens listed in Table 2 are prepared for triaxial (T1–T8) and consolidation (C1–C6) tests. All the tests were conducted according to the ASTM Standards. The moisture content of soil (*w*) was measured before and after consolidation. As expected, before consolidation initial *w* was equal to twice of LL. The undrained shear strength was also measured using a Torvane. All the results are summarized in Table 2.

Table 1. Soil properties of mixture

Soil property	75 % Sil-Co-Sil Silt + 25 % Kaolin
Specific gravity	2.65
Sand Content (%)	3
Plastic limit (PL)	22
Liquid limit (LL)	27
Soil type (Unified soil classification)	ML

Table 2. Properties of reconstituted soil samples

Property	Block sample 1	Block sample 2
Final moisture content (%)	24	24
Undrained shear strength	27	25

(kPa)		
Specimen preparation	C1,T1,T2,T3, T4,T8	C2,C3,C4,C5, C6, T5,T6,T7

3.2 One-dimensional consolidation tests

Six specimens (C1–C6 in Table 2) were prepared for one-dimensional consolidation tests. Soil samples from the Shelby tubes were inserted carefully into the consolidation moulds of 50 mm diameter and 20 mm height, and then the bottom and top surfaces were trimmed off to achieve proper seating. The moisture content of soil at this stage is also measured which represents the initial moisture content for consolidation test results analysis. The consolidation tests were conducted using pneumatic consolidation apparatus having a high accuracy digital display and data acquisition system.

The vertical stress is applied at a load increment ratio of 2 starting from 25 kPa. The samples were loaded up to 3,200 kPa with an unloading-reloading cycle at 400 kPa. Finally, the all the samples were unloaded to 25 kPa.

Figure 4 shows the v–logσ'_v curves for these six consolidation tests, where v is the specific volume (=1+e). In this figure, the initial void ratio (before application of 25 kPa vertical stress) is shown at σ'_v=1.0 kPa in the log scale. As shown, the slope of the curve gradually increases with σ'_v, indicating preconsolidation pressure around σ'_v=100 kPa. However, these curves do not converge to one line (normal compression line, NCL) at large vertical effective stresses, at least up to 3,200 kPa applied in these tests. The vertical difference between the consolidation curves at high stress level might be due to two reasons. First, it could be simply due to inaccurate measurement of initial void ratio. The difficulties in accurate measurement of initial void ratio have been reported in previous studies (e.g. Ponzoni et al. 2014). For their tests, Ponzoni et al. (2014) indicated the accuracy of ±0.05 in the measurement of specific volume. Secondly, the clay-silt mixture tested in the present study might have transitional behaviour as observed by previous researchers from one-dimensional consolidation tests on mixtures of sand, silt and clay (Martins et al. 2001; Nocilla et al. 2006; Ponzoni et al. 2014). Additional tests are required to identify the cause of this difference between the consolidation curves for the soil tested in this study.

3.3 Triaxial Compression tests

Similar to consolidated tests, triaxial tests specimens of 38 mm diameter and 76 mm height were prepared from the Shelby tube soil samples. Initial moisture content was also measured for each specimen from trimmed soil.

A series of consolidated drained and consolidated undrained triaxial compression tests was conducted as listed in Table 3. Tests were conducted using an advanced triaxial system as shown in Fig. 5. In this fully automated system, the cell and back pressures were controlled using the GDS pressure/volume controllers. The axial load was applied using a computer controlled loading system at a specified displacement rate. All the data such as back pressure, cell pressure, pore water pressure, volume change and axial displacement were recorded using a data acquisition system. Further details of test conditions are shown in Table 3.

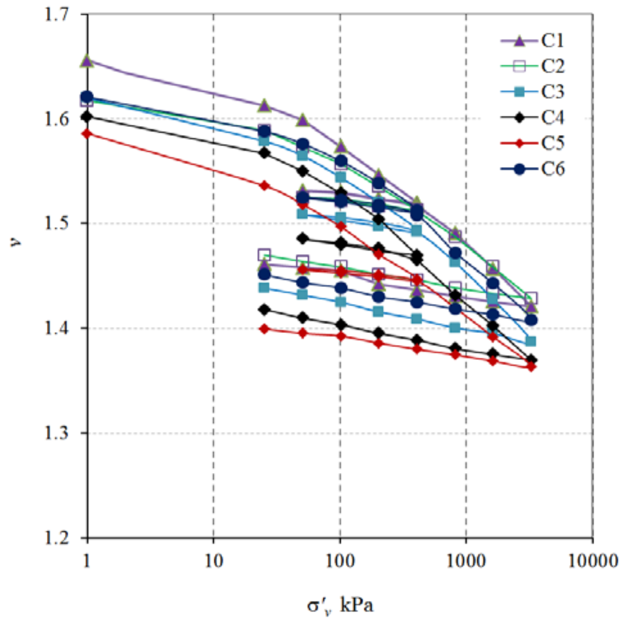

Figure 4. Consolidation test results

3.3.1 Consolidated drained triaxial tests

In tests T1–T4, the soil specimen was consolidated isotropically to the given confining pressure as shown in Table 3 and then sheared by compressing the specimen at 0.005 mm/min of vertical displacement as per ASTM recommendation ($\dot{\varepsilon}$ = 4%/10t_{90}, where t_{90} is the time required to achieve the 90% consolidation).

Figure 6 shows the stress–strain and volume change behaviour of soil during drained shearing. The deviatoric stress gradually increases and reaches the peak approximately at axial strain of 7–11%. After the peak, there is a slight decrease in deviator stress. The initial stiffness of the q–ε_1 curve increases with increase in confining pressure.

The volumetric strain versus axial strain curves in Fig. 6(b) show that the soil specimens first compress with increase in axial strain. For lower confining pressures (e.g. tests T1 and T2) the volume change behaviour changes after the maximum compression and then sample dilates (i.e. ε_v–ε_1 curves go up). In test T1, the ε_v–ε_1 curve does not become horizontal even at the maximum axial strain applied, which implies that the critical state may not be reached in this test. However, in tests T2 and T3 the ε_v–ε_1 curves become almost horizontal after some dilation. No significant dilation is observed in test T4 where the confining pressure is the maximum. Comparing these curves it can be concluded that dilative tendency of this soil decreases with increase in confining pressure, which is consistent with previous studies on sand (Jefferies and Been 2006).

A quick drop of q after the peak in the q–ε_1 plot in Test T3 and T4 might be due to strain localization in the failure plane, because any sharp change in volumetric strain was not observed at this level of strain in the ε_v–ε_1 plot. Notice that the volumetric strain is calculated from drained water which came out from the ends of the specimen. Therefore, local shearing along the failure plane may not be seen immediately from drainage of water from the sample. It is to be noted here that some researchers (e.g. Desrues and Viggiani 2004) also recognized such behaviour in sand, and inferred as localization effects which has been verified using stereo photogrammetry analysis.

Table 3. Triaxial test conditions

Test	Confining pressure, σ_c (kPa)	Type of shearing
T1	100	Drained
T2	200	Drained
T3	400	Drained
T4	640	Drained
T5	100	Undrained
T6	100	Undrained
T7	200	Undrained
T8	400	Undrained

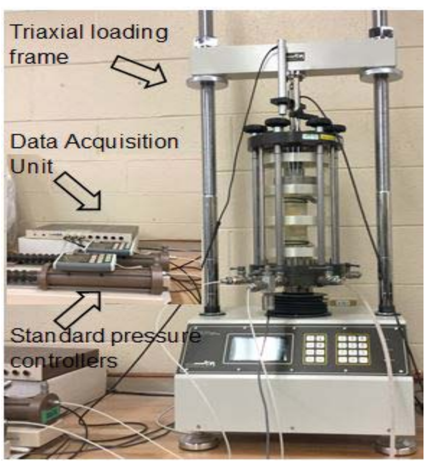

Figure 5. Automated GDS triaxial system

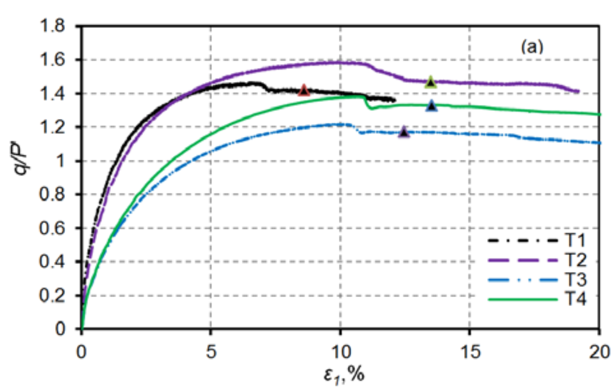

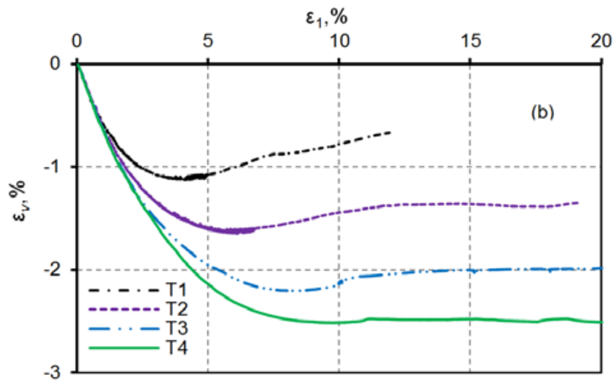

Figure 6. Stress–strain behaviour in consolidation drained tests: (a) deviatoric stress versus axial strain, (b) volumetric strain versus axial strain

3.3.2 Consolidated undrained traixial tests

In tests T5 and T8, the soil specimen was consolidated isotropically to the given confining pressure and then sheared by increasing axial stress in triaxial compression mode in undrained condition. However, in tests T6 and T7, the sample was first consolidated to 400 kPa and then unloaded isotropically to 100 and 200 kPa, respectively, meaning that, overconsolidated specimens were created in triaxial cell before shearing. The sample was then sheared in undrained condition by applying vertical displacement of 0.02 mm/min as per ASTM recommendation ($\dot{\varepsilon}$=4%/10t_{50}, where t_{50} is the time required to achieve the 50% consolidation).

Figure 7 shows the stress–strain and pore pressure change behaviour during undrained shearing. The deviatoric stress gradually increases and reaches the peak approximately at axial strain of 7–12%. All the specimens show a slight decrease in deviatoric stress after the peak, indicating less softening behaviour. The undrained elastic modulus (slope of the q–ε_1 curve) also increases with increase in confining pressure. Similar to drained tests, there is a sharp decrease of q after the peak in tests in T6 and T8, which could be again because of strain localization.

Figure 7(b) shows the developed of excess pore water pressure (u) during undrained shearing. The pore pressure is plotted by normalizing it with confining pressure (σ_c). In all the tests, pore water pressure increases with axial strain and then decreases, which indicate that the soil specimens initially contract and then dilate after some level of shearing. This could be better visualized from stress path of the samples presented in the following sections.

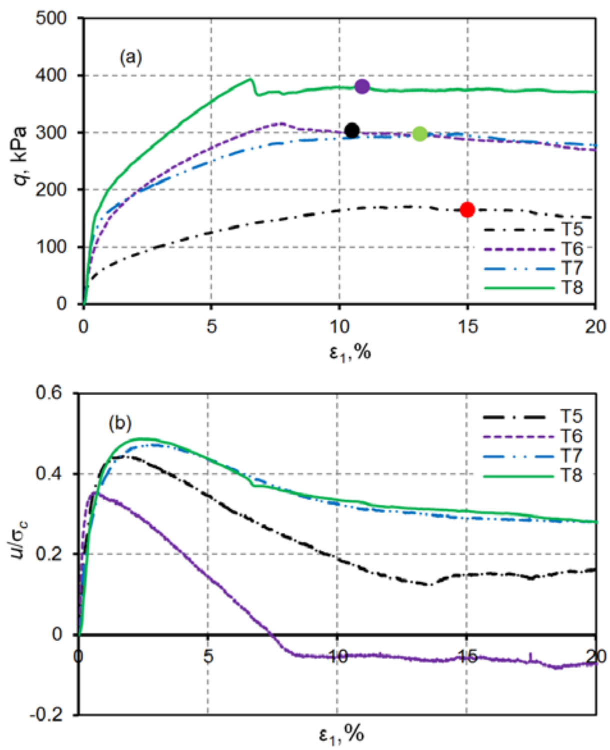

Figure 7. Stress–strain behaviour in consolidation undrained tests: (a) deviatoric stress versus axial strain, (b) normalized excess pore pressure versus axial strain

Although the soil specimens T5 and T8 were sheared from the maximum isotropic consolidation pressure applied in triaxial cell, these specimens also show some dilative behaviour. This could be because of two reasons. Firstly, the lab floor consolidation pressure is higher than the isotropic consolidation pressure in Test T5, which makes the soil specimen over-consolidated. However, in test T8 the sample was consolidated isotropically to 400 kPa, which is higher than the lab floor consolidation pressure. Therefore, the dilative behaviour of T8 is not due to over-consolidation. This could be due to initial void ratio of the specimen as commonly observed in dense sand which shows dilative behaviour although sand might be normally consolidated. Tests T6 and T7 are very similar except for the over-consolidation ratio (OCR) created in triaxial cell—OCR is 4 and 2 in T6 and T7, respectively. Comparing pore pressure variation in T6 and T7 it can be shown that sample T6 shows more dilative behaviour than T7 because the pore pressure decrease in T6 is higher than T7 and after ε_1~7.5% the pore pressure is negative in T6 which has higher OCR. In other words, the stress–strain behaviour of this clayey silt is not exactly same as clay or sand, rather it depends significantly on OCR and initial void ratio, meaning that the behaviour is somewhere between clay and sand.

3.3.3 Effective stress path

Figure 8 shows the effective stress path of the soil specimens during undrained shearing. In tests T5 and T8, the specimens show contractive behaviour initially and then dilative behaviour with a phase change similar to dense sand. However, in the overconsolidated specimens T6 and T7 the undrained stress paths initially move almost vertically, indicating elastic behaviour, followed by a dilation tail similar to T5 and T8. Although authors recognize that it is very difficult to identify the critical state condition from these tests results because the deviatoric stress and pore pressure do not become constant even at large strains. The approximate location of the critical state is shown by the circles in this figure. The specimens T5 and T8, which were not overconsolidated in triaxial cell, reached almost the same stress ratio at the critical state (q/p'=1.1). However, for the overconsolidated soil specimens q/p' could be greater than this value,1.3 in T7 and 1.5 in T6,which means that OCR also significantly influence the behavior of this clayey silt.

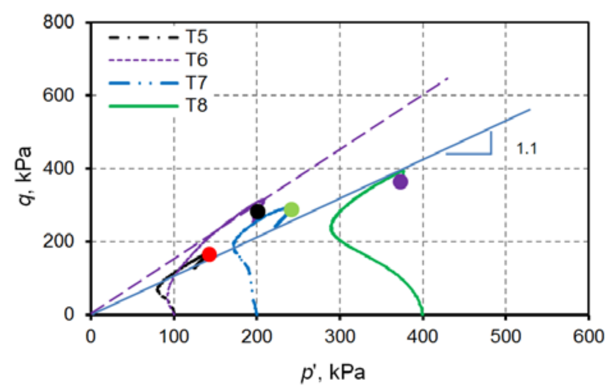

Figure 8. Effective stress path for consolidated undrained triaxial tests

The effective stress paths for the drained tests are shown in Fig. 9. As shown in Fig. 6(a) the deviator stress reaches the peak and then decreases. Moreover, the volumetric strain change with axial strain does not become zero at large strains (Fig. 6b); therefore, the triangles shown in Fig. (6a) are assumed to be at the critical state. The stress state (p',q) at this condition is shown in Fig. 9 by triangles. An average line drawn through these triangles gives the slope of the critical state line of 1.25. For comparison with M obtained from undrained tests without any pre-consolidation in triaxial cell (the lower line in Fig. 8), a line having slope of 1.1 is also drawn in this figure. As shown, the drained tests give slightly higher M.

In summary, the triaxial test results show that there is a discrepancy between the values of M obtained from drained and undrained tests. Nocilla et al. (2006) also recognized such difference in their test on Italian silt mixed with clay.

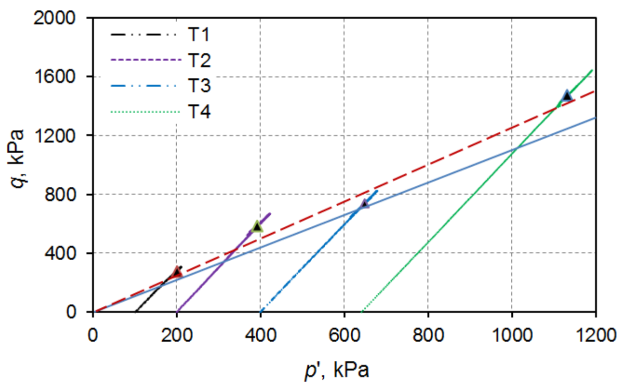

Figure 9. Effective stress path for consolidated drained triaxial tests

4 CONCLUSIONS

From previous studies it is found that frost susceptibility of 75% sil-co-sil silt and 25% kaolin mixture is comparable to Calgary silt, and therefore this mixture has be used for centrifuge modeling of frost heave behaviour under chilled gas pipelines. In the present study, stress–strain behaviour of this frost susceptible soil is examined from a series of one-dimensional consolidation, triaxial compression tests. One-dimensional consolidation tests show that the consolidation curves do not converge to one line at large vertical effective stress, although the difference between these curves is not very significant. Undrained triaxial compress tests show dilative tendency at large strains. The slope of the critical state line is not constant but varies with drainage condition during shearing (drained or undrained). In other words, unique critical state line the p'–q plane was not obtained for this soil.

Finally, it is to be noted here that above conclusions have been drawn from a limited number of tests. Additional experimental investigation is required for better explanation of the test results presented above.

ACKNOWLEDGEMENTS

The works presented in this paper have been supported by the Research and Development Corporation of Newfoundland and Labrador (RDC) and NSERC. The authors also express their sincere thanks to Shantanu Kar and Anup Fouzder for their help with laboratory testing.

REFERENCES

Andersland, O.B. and Ladanyi, B. 2004. *Frozen ground engineering*, 2nd ed., John Wiley & Sons, Hoboken, New Jersey, USA, 363p

Clark, J.I. and Phillips, R. 2003. Centrifuge modeling of frost heave of Arctic gas pipelines, *8th International Permafrost Conference,* Balkema Publishers, Zurich, Switzerland, 1:152–156.

Desrues, J. and Viggiani, G. 2004. Strain localization in sand: an overview of the experimental results obtained in Grenoble using stereophotogrammetry, *Int. J. Numer. Anal. Meth. Geomech.,* 28:279–321.

Jefferies, M. and Been, K. 2006. *Soil Liquefaction: A Critical state approach*, 1st ed., Taylor & Francis, New York, NY, USA, 479p.

Ketcham, S., Black, P. and Pretto, R. 1997. Frost heave loading of constrained footing by centrifuge modelling, J. Geotech. Eng., ASCE, 123(9):874–881.

Konrad, J. and Morgenstern, N. 1984. Frost heave prediction of chilled pipelines buried in unfrozen soils, *Canadian Geotechnical Journal*, 21(1):100–115.

Konrad, J. and Shen, M. 1996. 2-D frost action modeling using the segregation potential of soils, *Cold regions science and technology*, 24(3):263-278.

Ladanyi, B. and Shen, M. 1993. Freezing pressure development on a buried chilled pipeline, *2nd Int. Symp. on frost in geotechnical engineering*, Anchorage, AK.,23-33.

Martins, F.B., Bressani, L.A., Coop, M.R. and Bica, A. V.D. 2001. Some aspects of the compressibility behaviour of clayey sand, *Canadian Geotechnical Journal*, 38:1177–1186.

Michalowski, R.L. and Zhu, M., 2006. Frost heave modelling using porosity rate function, *Int. J. Numer. Anal. Meth. Geomech.* ,30(8): 703–722.

Morgan, V., Clark, J.I., and Hawlader, B. 2004. Modeling of frost heave of gas pipelines in Arctic conditions, *International Conference on Terrain and Geohazard Challenges Facing Onshore Oil and Gas Pipelines*, Thomas Telford, London, 1: 417–427.

Morgan, V., Hawlader, B., and Zhou, J. 2006. Mitigation of frost heave of chilled gas pipelines using temperature cycling, *6th International Pipeline Conference*, ASME, Calgary, 1:927–931.

Nishimura, S., Gens, A., Olivella, S. and Jardine, R. J. 2009. THM-coupled finite element analysis of frozen soil: formulation and application, *Geotechnique*, 59(3): 159–171.

Nixon, J. 1991. Discrete ice lens theory for frost heave in soils, *Canadian Geotechnical Journal*, 28:843–859.

Nocilla, A., Coop, M. and Colleselli, F. 2006. The mechanics of an Italian silt: an example of transitional behaviour, *Geotechnique*, 56(4):261–271.

Piercey, G., Volkov, N., Phillips, R. and Zakeri, A., 2011. Assessment of Frost Heave Modelling of Cold Gas Pipelines, *Pan-Am CGS Geotechnical conference*,8.

Ponzoni, E., Nocilla, A., Coop, M.R. and Colleselli, F. 2014. Identification and quantification of transitional modes of behaviour in sediments of Venice lagoon, *Geotechnique*, 64(9):694–708.

Shen, M., and Ladanyi, G. 1991. Soil-pipe interaction during frost heaving around a buried chilled pipeline, *6th International Cold Regions Engineering Conference*, West Lebanon, NH. , 11–21.

Yang, D. and Goodings , D.J. 1998. Climatic Soil Freezing Modelled in Centrifuge, *Journal of Geotech. and Geo-environmental Eng. ASCE*, 124(12): 1186-1194.